# OGO-C ORIENTATION STUDY

by

Paul E. Dimotakis

SPACE RADIATION LABORATORY

INTERNAL REPORT NO. 9

California Institute of Technology

Pasadena, California

## ABSTRACT

The aim of this calculation is to determine the orientation of the OGO-C spacecraft after the altitude Control System ceased to function properly. The problem is approached by approximating the sun aspect angle $\alpha$ by

$$\cos \alpha = \cos \beta \cos \gamma + \cos A \sin \beta \sin \gamma$$

where A, $\beta$, and $\gamma$ are determined for each interval during which it was possible to analyze the Housekeeping data. A and $\gamma$ were assumed to vary linearly within each interval according to

$$A = \omega_A (t - t_o) + A_o$$

$$\gamma = \omega_\gamma (t - t_o) + \gamma_o$$

and $\beta$ was found to be almost constant within each interval. Values for the above parameters were derived from the Housekeeping data and are listed in Table I for each of 10 intervals. Figures 11-17 are plots of the data and the above equation using the parameters in Table I. Using the analytical form of the fit for $\alpha$ and data pertaining to the position of the spacecraft from the Attitude-Orbit Tapes, it is possible to solve for any angle between the Z-axis of the spacecraft and the axes of any coordinate system.

# OGO-C ORIENTATION STUDY

## The General Problem

OGO-C was designed to orbit with the body Z-axis directed towards the center of the earth. Due to a malfunction of the horizon scanners, however, the attitude control gas was expended during the first few days of operation. Thereafter, the spacecraft oriented itself subject to external forces alone. The present work is an attempt to estimate the angular deviation of the body Z-axis from the geocentric vector, $\delta$. Once this angle ($\delta$) is known such things as the right ascension and declination of the Z-axis can be calculated with the help of the attitude orbit tapes, as will be discussed later.

Housekeeping information and gravity gradient considerations indicate that the spacecraft Z-axis is precessing about the orbit normal ($\vec{L}$) with a slowly varying period of approximately 40 orbits. The following discussion and final calculation are based on this assumption whose validity will be discussed later. (see figure 1).

The problem of determining the angle between the Z-axis and the geocentric vector is essentially the solution of a three-dimensional configuration of the following vectors:

(i) Orbit Normal ($\vec{L}$); a unit vector defined to correspond in sign with the sense in which the spacecraft revolves about the earth. (see figure 1)

(ii) Sun Vector ($\vec{S}$): a unit vector in the direction of the sun.

(iii) Geocentric Vector ($\vec{G}$): a unit vector in the direction of the center of the earth.

(iv) The positive body Z-axis ($\vec{Z}$)

If we define the quantities A, $\Phi$, $\Delta$, $\beta$ as in Figure 3, then we can solve the spherical triangle (see appendix A) defined by the unit vectors $\vec{G}$, $\vec{L}$, $\vec{Z}$ for the angle $\delta$, to get

$$\cos \delta = \sin \beta \left[\cos A \cos \Phi + \sin A \sin \Phi\right] \qquad (3)$$

(equation (3), figure 3). It is thus apparent that the following quantities must be calculated in order to compute the angle $\delta$:

(i) $\beta$: The (L, Z) angle, assumed to be the slowly varying precession cone half-angle.

(ii) A: The dihedral angle ($\hat{SLZ}$) whose rate of change corresponds to the rate of precession of the $+\vec{Z}$ axis about $+\vec{L}$.

(iii) $\Phi$: The dihedral angle ($\hat{SLG}$).

The first two of these quantitites are calculated with reference to the angle subtended between the $+\vec{Z}$ body axis and the sun vector $\vec{S}$, hereafter referred to as the sun aspect angle $\alpha$. The last angle does not depend on the orientation of the spacecraft and is calculable from the Attitude Orbit Tape.

The Sun-Aspect-Angle

The sun-aspect-angle can occasionally be calculated from housekeeping data. Ideally the y-axis of the panel coordinates points towards the sun (see figure 4). A measure of the deviation from the ideal panel orientation is afforded by means of words A-10 and A-11 of the housekeeping subcomm frames. Geometrically they are defined as follows:

(i) A-10: Supplement to the arc subtended between the panel X-axis and the sun vector.

(ii) A-11: Supplement to the arc subtended between the panel Z-axis and the sun vector. (see also figure 2)

In addition to these, we are given the angle between the panel Z-axis and the body Z-axis through housekeeping subcomm words A-12, A-13, and A-23, (arrays).

We can then solve triangle $\vec{S}_B$, $\vec{Z}_p$, $\vec{S}$ (figure 4) to get

$$\cos (Z_p, S) = \cos (S, S_B) \cos (S_B, Z_p) + \cos (S \hat{S}_B Z_p) \sin (S, S_B) \sin (S_B, Z_p)$$

$$\therefore \quad (S_B, Z_p) = \arccos \frac{\cos (Z_p, S)}{\cos (S_B, S)} \qquad (4)$$

From triangle $\vec{Z}_B$, $\vec{S}_B$, $\vec{S}$, the sun aspect angle is given by

$$\cos \alpha = \cos (Z_B, S_B) \cos (S_B, S) + \cos (Z_B \hat{S}_B S) \sin (Z_B S_B) \sin (S_B, S)$$

but $(Z_B, S_B) = (Z_B, Z_p) - (S_B, Z_p)$

$$\therefore \quad \cos \alpha = \cos \left[ (Z_B, Z_p) - (S_B, Z_p) \right] \cos (S_B, S) \qquad (5)$$

in which we know all the quantities on the right hand side because

(i) $(Z_B, Z_p)$ is the array angle defined by A-12, A-13, and A-23.

(ii) $(S_B, Z_p)$ is calculated from equation (4) in which:

(a) $(Z_p, S)$ is the supplement to A-11

(b) $(S_B, S)$ is A-10

(iii) $(S_B, S)$ is A-10

and it would appear that we can easily calculate the sun aspect angle whenever A-10, A-11, A-12, A-13 and A-23 are well defined. A-10 and A-11, however, are essentially light sensitive indicators from whose calibrated

response the angle of incidence can be inferred as a function of the intensity of the incident light. If the sun were the only source of light, then the calibrated response would indeed provide a unique definition of the direction of the sun vector. The spacecraft, however, being free to point in all directions, is at times bathed in light coming from the illuminated side of the earth. Consequently, if we were to attribute the direction of the incident intensity to the sun alone, we would assign a direction to the sun vector corresponding to the weighted vector sum of the directions of all the possible sources of light that the sensors see. (see figure 5). This would appear to displace the sun in a periodic way, with characteristic times corresponding to the orbit and one half the spin period. This phenomenon has been referred to in previous literature dealing with the attitude control as the "albedo effect". It is virtually impossible to arrive at a theoretical means of subtracting this component of incident light. Reflectivity, for instance, would be a function of the position of the subsatellite point, the altitude of the spacecraft, the time of day, Los Angeles smog, cloud formations, and other phenomena.

One approach to this problem is to find positions in the orbit where the effect can be expected to be least significant. Since the satellite orbits at an average height which is not small compared to the earth's radius, there is a certain interval between the time when the subsatellite point enters the dark side of the earth and the time when the spacecraft enters the eclipsed region (if any) of the orbit (arcs AB and CD in figure 6). During this time interval the solid angle subtended by the illuminated portion of the earth is considerably less than at other times when the satellite sees the sun. Such intervals occur before and after each eclipse. If the satellite never goes into eclipse, it is in this

favorable condition approximately half the time.

If we define (figure 6)

A: The point in the orbit after which the subsatellite point is in darkness.

B: The point in the orbit after which the spacecraft is in eclipse.

C: The point in the orbit at which the spacecraft leaves eclipse.

D: The point at which the subsatellite point is on the day side of the earth.

P: The position vector from the center of the earth to the satellite.

S: The sun vector.

R: The earth's radius.

then it is clear that points A and D occur at $(P, S) = 90^{o}$. If we assume that the vector to the sun from the center of the earth is parallel to the sun vector to the sun from the center of the earth is parallel to the sun vector from the satellite, then the satellite is eclipsed if

$$\sin (P, S) < \frac{R}{R + H}$$

where H is the spacecraft height above the earth at that point.

H and (P, S) are given on the attitude orbit tape every sixty seconds. For R we used 6400 kilometers as a bonus radius of the earth. Then the criterion for minimum albedo contribution is

$$\frac{R}{R + H} < \sin (P, S) < 1; \quad (P, S) > 90^{o} \qquad (6)$$

Plots of the raw sun aspect angle data (as computed with equation (5)) demonstrate these effects (see figures 7, 8, 9, 10 and appendix B). The

numbers scaling the axes are to be multiplied by the corresponding scaling factors. Thus figure 7 is scaled from day 19.81 to day 20.05 (January 19, 1966, 7:30 p.m. to January 20, 1966, 1:12 a.m.) and from 0 to 180 degrees. The gaps in the data occur for various reasons:

(i) data missing on the tape

(ii) indicators outside calibrated limits. This problem becomes the main reason for the scarcity of data as soon as the angle between the orbit normal and the satellite-sun line is greater than about 40 degrees or less than 140 (see figure 20).

(iii) inconsistent definition of array angle through words A-12, A-13, A-23.

During the period when the spacecraft is in eclipse the arrays remain locked at the angle they were just prior to eclipse. The sun sensors, however, give zero or nearly zero as a reading. The S.A.A. as computed from these arrays is dependent on the position in the spin cycle that the spacecraft was when it entered eclipse. This effect can be seen as the regions of constant sun aspect angle on figures 7, 8, 9, 10. See also appendix B for an example of the actual data during eclipse.

The effect of the albedo interference is seen to be less just before and just after each eclipse, in agreement with the above discussion. The periodic modulation of the sun aspect angle data due to the albedo effect has been interpreted as a nutation with a period equal to that of the orbit. We believe that it is merely a consequence of the albedo effect which seems to explain it quite adequately. There are no obvious torque transients that would cause such a persistent nutation. The data points on figures 11, 12, 13, 14, 15, 16, 17 are the sun aspect angle averages

during the favorable intervals defined through equation (6). There is an occasional small disagreement between the time-span of an eclipse, as predicted by the attitude orbit tape and the time as suggested by the data. This sometimes allows points corresponding to the flat regions during eclipse (figures 7-10) to be included in the average data. For this reason, all data points more than two standard deviations away, are ignored and the average is computed without them. The crosses correspond to error bars associated with the particular average. The vertical extent corresponds to the standard deviation of the mean, while the length of the horizontal bar is 2/3 of the time interval over which the average was computed. Error bars in either direction of less than 0.05" are replaced by lines of that length. The vertical axis is scaled to 180 degrees while the horizontal axis is in days of the year. Thus figure 11 includes data from October 13 to October 22. Day counts for figures 11 and 12 are from 1965. The rest are from 1966.

The continuous curve, which is also plotted, can be drawn through these points if we solve the equations of "motion". The vectors $\vec{L}$, $\vec{S}$, and $\vec{Z}$ form a spherical triangle which can be solved for the sun aspect angle $\alpha$ to get (see figure 18)

$$\cos \alpha = \cos \beta \cos \gamma + \cos A \sin \beta \sin \gamma \qquad (7)$$

where the quantities $\alpha$, $\beta$, $\gamma$ and A are defined on figure 18. If the spacecraft is indeed precessing about the orbit normal, then the following should be true over a short interval

(i) $\beta$, the angle between $\vec{L}$ and $\vec{Z}$ should be approximately constant (precession-cone half-angle).

(ii) A, the dihedral angle ($\hat{SLZ}$), should vary with a constant angular frequency (rate of precession).

Since $\gamma$ is the angle subtended between the orbit normal and the sun vector, it changes slowly at the rate at which the orbit plane precesses with respect to the sun vector. If, therefore, the assumption that the spacecraft is precessing about the orbit normal is valid, the solutions to equation (7), with the following approximations,

(i) $\beta \tilde{\approx}$ constant

(ii) $\gamma \tilde{\approx} \omega_\gamma (t-t_o) + \gamma_o$

(iii) $A \tilde{\approx} \omega_A (t-t_o) + A_o$

should fit the data well.

The continuous curves on figures 11, 12, 13, 14, 15, 16, 17 are a plot of equation (7) to which the following were supplied:

(1) t start
(2) t end — range of validity (days)
(3) $\beta$ in radians
(4) $\omega_\gamma$ in radians per day
(5) $\gamma_o$ in radians
(6) $\omega_A$ in radians per day
(7) $A_o$ in radians
(8) $t_o$ in days

The final values are then defined by a trial and error procedure. The values that were used to calculate the continuous curves are listed in Table I. We consider the success of the fits to be sufficient evidence in support of the assumption that the spacecraft is precessing, with a slowly varying period of $2\pi/\omega_A$, about the orbit normal.

From these numbers $\beta$ can be used as such, while $\omega_A$, $A_o$ and $t_o$ can be used to calculate A. These are 2 of the 3 angles to be used in equation (3)

to calculate $\delta$ , the (Z, G) angle. The third angle is the dihedral angle (SLG), discussed below.

The (SLG) dihedral angle (see Figure 3)

From the attitude orbit tapes the X, Y and Z components of the $\vec{L}$, $\vec{S}$, $\vec{G}$ unit vectors can be calculated as follows:

(i) $\vec{L}$: Words 43, 44, 45 of the attitude orbit tape record correspond to the ideal OPEP pitch axis which is the negative of what we have defined as $\vec{L}$ (see page 4 and Table II). $\vec{L}$ as used here is the negative $Y_{EI}$.

(ii) $\vec{S}$: Words 14, 15, 16 of the attitude orbit tape give the three components of the solar vector. The sun vector that is used here is merely the normalized vector corresponding to words 14, 15, 16.

(iii) $\vec{G}$: Since this is the ideal main body +Z-axis, words 28, 29, 30 correspond exactly to $G_X$, $G_Y$, $G_Z$.

Using $\vec{L}$ and $\vec{S}$ we can define a vector $\vec{C}$ (see figure 21) along the intersection of the orbit plane and the $\vec{L}$, $\vec{S}$ plane. Then, by definition of a dihedral angle,

$$\Phi = (C, G)$$

then $\cos \Phi = \vec{C} \cdot \vec{G} / |\vec{C}|$

and $\sin \Phi = + \sqrt{1 - \cos^2 \Phi}$ if $\vec{L} \cdot \vec{C} \times \vec{G} > 0$

$= - \sqrt{1 - \cos^2 \Phi}$ if $\vec{L} \cdot \vec{C} \times \vec{G} < 0$

The sine and cosine of $\Phi$ can then be used to calculate $\delta$ in equation (3).

The (Z, G) angle ($\delta$)

We can now solve equation (3) to obtain $\delta$ as often as $\vec{S}$, $\vec{G}$, and $\vec{L}$ are given in the Attitude-Orbit-Tape. A plot of this result appears in Figure 22. The second curve is a plot of the half-angle "h" of the cone that is subtended by the earth (see Figure 23).

Right ascension and declination of the body Z-axis

As a result of the above calculation, we know the angle subtended between the body Z-axis and $\vec{L}$, $\vec{S}$, and $\vec{G}$. When these are not coplanar it becomes possible, by a simple transformation of coordinates, to obtain the x, y, z components of the body Z-axis.

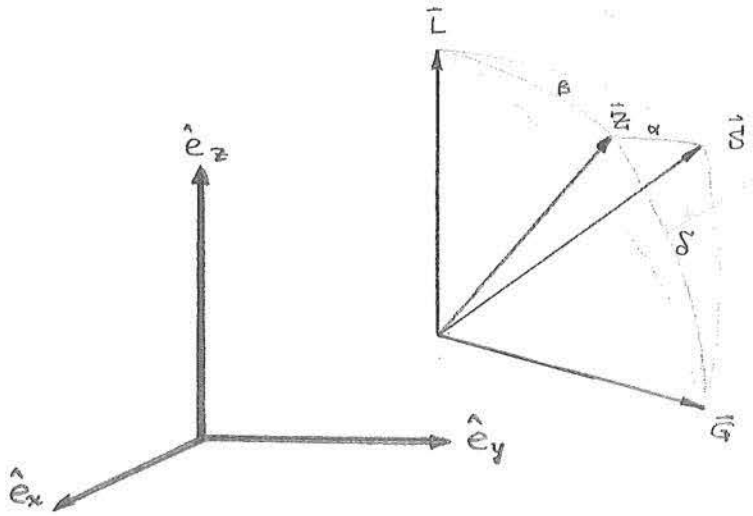


$\beta \equiv (L, Z)$
$\alpha \equiv (Z, S)$
$\delta \equiv (Z, G)$

FIGURE 24.

Then

$$Z_x = (\vec{Z} \cdot \vec{L})\, L_x + (\vec{Z} \cdot \vec{G})\, G_x + (\vec{Z} \cdot \vec{S})\, S_x$$

$$Z_y = (\vec{Z} \cdot \vec{L})\, L_y + (\vec{Z} \cdot \vec{G})\, G_y + (\vec{Z} \cdot \vec{S})\, S_y$$

$$Z_z = (\vec{Z} \cdot \vec{L})\, L_z + (\vec{Z} \cdot \vec{G})\, G_z + (\vec{Z} \cdot \vec{S})\, S_z$$

or, using the definitions in Figure 24

$$\begin{pmatrix} Z_x \\ Z_y \\ Z_z \end{pmatrix} = \overset{\text{from Attitude-Orbit-Tape}}{\begin{pmatrix} L_x & G_x & S_x \\ L_y & G_y & S_y \\ L_z & G_z & S_z \end{pmatrix}} \cdot \begin{pmatrix} \cos\ \beta \\ \cos\ \delta \\ \cos\ \alpha \end{pmatrix}$$

Since $\vec{Z}$, as calculated, is a unit vector, we can compute the polar and azimuthal angle from which right ascension and declination are easily derivable.

From Figure 25

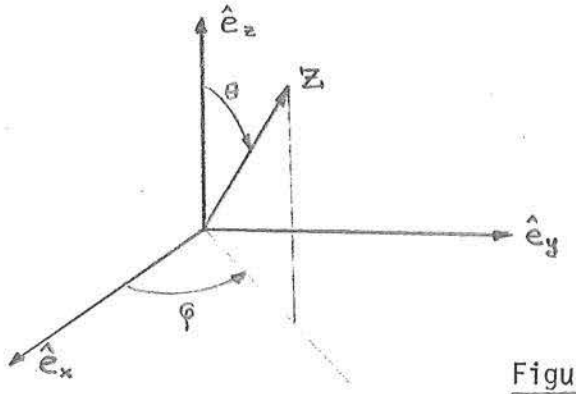


Figure 25.

$$\theta = \text{arc cos } (Z_z)$$

and

$$\varphi = \left\{ \begin{array}{l} \text{arc cos } (Z_x/\sin\ \theta) \\ \\ \text{arc sin } (Z_y/\sin\ \theta) \end{array} \right\} \quad \text{unique definition of } \varphi$$

# APPENDIX A

## Spherical Trigonometry

A spherical triangle is defined on the surface of a sphere by the intersection of three major circles.

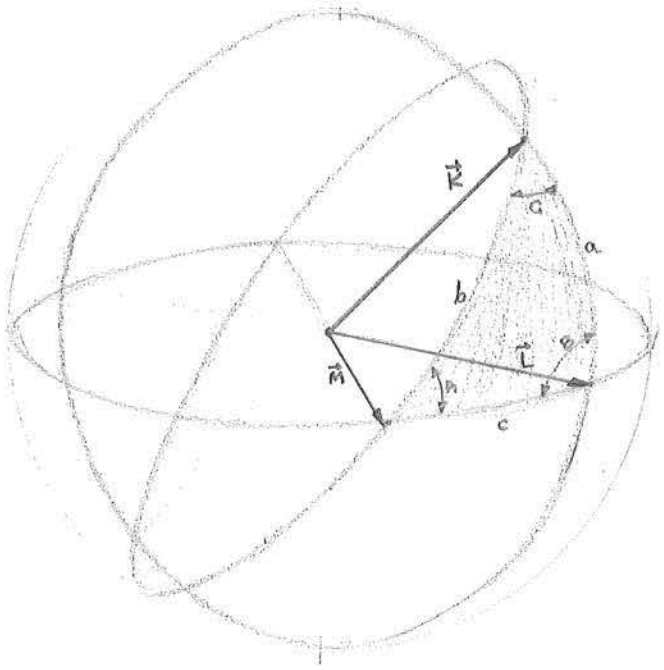


Figure A-1.

Let a, b, c be the arc segments that form the three sides and A, B, C the correspondingly opposite dihedral angles.

We then have the following relations

$$\frac{\sin a}{\sin A} = \frac{\sin b}{\sin B} = \frac{\sin c}{\sin C} \qquad (1)$$

$$\cos a = \cos b \cos c + \cos A \sin b \sin c$$

$$\cos A = \cos B \cos C + \sin B \sin C \cos a$$

Since most of the spherical triangles encountered are defined by means of three vectors, the following notation will alternatively be used (see Figure A-1).

$a = (K, L)$ : arc subtended between $\vec{K}$ and $\vec{L}$

$A = (\hat{KML})$ : angle subtended between $\vec{K}$, $\vec{M}$ and $\vec{M}$, $\vec{L}$ planes.

# APPENDIX B

## S.A.A. Data

The sun aspect angle is calculated on the basis of equation (5) as explained in the text. In the two following pages is a sample output of the words A-10, A-11, A-12, A-13 at a time when the data are reasonably good. The second page is an example of what the data look like during an eclipse.

1. RC: record number on the tape
2. HR, MN, MSECS } time of readout
3. first data column is the binary output (converted to a decimal) corresponding to the channel number ($1 \leq \text{data} \leq 256$).
4. The column under the word headings (A-10, A-11, A-12, A-13) is the decoded output via the calibration matrices given in appendix C. The columns labeled I.Q. give an indication of the quality of the particular number as follows:

| Words | I.Q. | Meaning |
|---|---|---|
| A-10, A-11 | 0 | data missing |
| | 1 | fine sensor used* |
| | 2 | coarse sensor used |
| | 3 | coarse sensor used (A23 = 0) |
| | 4 | coarse sensor used (A23 missing) |
| | 5 | coarse sensor used (A23 nonsense) |
| | 6 | data off scale (Low) |
| | 7 | data off scale (High) |
| A-12, A-13 | 0 | data missing |
| | 1 | data on scale |
| | 2 | data off scale |
| | 3 | data inconclusive (A-12 = 0) |

*see Appendix C

In the final calculation an I.Q. of 1 or 2 was required of words A-10 and A-11 while an I.Q. of 1 was required of either A-12 or A-13. If these requirements were not met, $\alpha$ (the sun aspect angle in degrees) which appears on the last column, was set to 690.0 and ignored thereafter.

PAGE NO. 3 FILE NO. 1 DAY NO. 20

| RC | HR | MN | MSECS | | A10 | IQ | HR | MN | MSECS | | A11 | IQ | HR | MN | MSECS | | A12 | IQ | HR | MN | MSECS | | A13 | IQ | ALPHA |
|---|---|---|---|---|---|---|---|---|---|---|---|---|---|---|---|---|---|---|---|---|---|---|---|---|---|
| 101 | 10 | 9 | 55366 | 127 | 1.40 | 2 | 10 | 9 | 50122 | 129 | 0.92 | 2 | 10 | 9 | 45226 | 18 | 0. | 2 | 10 | 9 | 45514 | 62 | 245.90 | 1 | 154.9 |
| 102 | 10 | 10 | 32170 | 176 | 15.45 | 2 | 10 | 10 | 26986 | 130 | 1.19 | 2 | 10 | 10 | 22090 | 18 | 0. | 2 | 10 | 10 | 22378 | 67 | 248.40 | 1 | 152.7 |
| 103 | 10 | 11 | 9034 | 237 | 28.23 | 2 | 10 | 11 | 3650 | 123 | -0.73 | 2 | 10 | 10 | 58954 | 18 | 0. | 2 | 10 | 10 | 59242 | 101 | 264.00 | 1 | 151.3 |
| 104 | 10 | 11 | 45898 | 232 | 27.18 | 2 | 10 | 11 | 40714 | 125 | -0.18 | 2 | 10 | 11 | 35818 | 19 | 0. | 2 | 10 | 11 | 36106 | 155 | 287.00 | 1 | 148.2 |
| 105 | 10 | 12 | 22762 | 179 | 16.08 | 2 | 10 | 12 | 17578 | 126 | -0.09 | 2 | 10 | 12 | 12682 | 20 | 0. | 2 | 10 | 12 | 12970 | 174 | 295.10 | 1 | 150.4 |
| 106 | 10 | 12 | 59625 | 116 | -3.00 | 2 | 10 | 12 | 54441 | 128 | 0.65 | 2 | 10 | 12 | 49545 | 21 | 0. | 2 | 10 | 12 | 49833 | 182 | 298.60 | 1 | 151.9 |
| 107 | 10 | 13 | 36489 | 55 | -17.49 | 2 | 10 | 13 | 31305 | 126 | -0.09 | 2 | 10 | 13 | 26409 | 20 | 0. | 2 | 10 | 13 | 26697 | 173 | 294.70 | 1 | 150.0 |
| 108 | 10 | 14 | 13353 | 3 | -27.99 | 2 | 10 | 14 | 8169 | 130 | 1.19 | 2 | 10 | 14 | 3273 | 19 | 0. | 2 | 10 | 14 | 3561 | 143 | 281.90 | 1 | 150.2 |
| 109 | 10 | 14 | 50217 | 18 | -24.97 | 2 | 10 | 14 | 45033 | 130 | 1.19 | 2 | 10 | 14 | 40137 | 18 | 0. | 2 | 10 | 14 | 40425 | 97 | 262.10 | 1 | 153.5 |
| 110 | 10 | 15 | 27081 | 100 | -8.41 | 2 | 10 | 15 | 21897 | 130 | 1.19 | 2 | 10 | 15 | 17001 | 18 | 0. | 2 | 10 | 15 | 17289 | 72 | 250.80 | 1 | 158.0 |
| 111 | 10 | 16 | 3945 | 156 | -11.26 | 2 | 10 | 15 | 58761 | 126 | -0.09 | 2 | 10 | 15 | 53865 | 18 | 0. | 2 | 10 | 15 | 54153 | 62 | 245.90 | 1 | 153.6 |
| 112 | 10 | 16 | 40809 | 232 | 27.18 | 2 | 10 | 16 | 35625 | 124 | -0.45 | 2 | 10 | 16 | 30729 | 18 | 0. | 2 | 10 | 16 | 31017 | 81 | 254.80 | 1 | 149.4 |
| 113 | 10 | 17 | 17672 | 246 | 30.11 | 2 | 10 | 17 | 12488 | 128 | 0.65 | 2 | 10 | 17 | 7592 | 19 | 0. | 2 | 10 | 17 | 7880 | 139 | 280.20 | 1 | 148.0 |
| 114 | 10 | 17 | 54536 | 194 | 19.22 | 2 | 10 | 17 | 49352 | 124 | -0.45 | 2 | 10 | 17 | 44456 | 20 | 0. | 2 | 10 | 17 | 44744 | 176 | 296.00 | 1 | 147.7 |
| 115 | 10 | 18 | 31400 | 121 | 0. | 2 | 10 | 18 | 26216 | 125 | -0.18 | 2 | 10 | 18 | 21320 | 21 | 0. | 2 | 10 | 18 | 21608 | 189 | 301.50 | 1 | 148.3 |
| 116 | 10 | 19 | 8264 | 89 | -10.63 | 2 | 10 | 19 | 3080 | 131 | 1.47 | 2 | 10 | 18 | 58184 | 21 | 0. | 2 | 10 | 18 | 58472 | 187 | 300.70 | 1 | 149.1 |
| 117 | 10 | 19 | 45128 | 30 | -22.54 | 2 | 10 | 19 | 39944 | 130 | 1.19 | 2 | 10 | 19 | 35048 | 20 | 0. | 2 | 10 | 19 | 35336 | 162 | 290.00 | 1 | 151.0 |
| 118 | 10 | 20 | 21992 | 11 | -26.38 | 2 | 10 | 20 | 16808 | 132 | 1.75 | 2 | 10 | 20 | 11912 | 19 | 0. | 2 | 10 | 20 | 12200 | 112 | 268.90 | 1 | 153.5 |
| 119 | 10 | 20 | 58856 | 48 | -18.91 | 2 | 10 | 20 | 53672 | 130 | 1.19 | 2 | 10 | 20 | 48776 | 18 | 0. | 2 | 10 | 20 | 49064 | 67 | 248.40 | 1 | 150.7 |
| 120 | 10 | 21 | 35719 | 135 | 4.59 | 2 | 10 | 21 | 30535 | 126 | -0.09 | 2 | 10 | 21 | 25639 | 18 | 0. | 2 | 10 | 21 | 25927 | 53 | 241.50 | 1 | 151.3 |
| 121 | 10 | 22 | 12583 | 194 | 19.22 | 2 | 10 | 22 | 7399 | 124 | -0.45 | 2 | 10 | 22 | 2503 | 18 | 0. | 2 | 10 | 22 | 2791 | 68 | 248.90 | 1 | 152.1 |
| 122 | 10 | 22 | 49447 | 255 | 31.99 | 2 | 10 | 22 | 44263 | 124 | -0.45 | 2 | 10 | 22 | 39367 | 18 | 0. | 2 | 10 | 22 | 39655 | 106 | 266.30 | 1 | 147.9 |
| 123 | 10 | 23 | 26311 | 247 | 30.32 | 2 | 10 | 23 | 21127 | 124 | -0.45 | 2 | 10 | 23 | 16231 | 20 | 0. | 2 | 10 | 23 | 16519 | 166 | 291.70 | 1 | 143.6 |
| 124 | 10 | 24 | 3175 | 177 | 15.66 | 2 | 10 | 23 | 57991 | 124 | -0.45 | 2 | 10 | 23 | 53095 | 20 | 0. | 2 | 10 | 23 | 53383 | 193 | 303.20 | 1 | 142.3 |
| 125 | 10 | 24 | 40039 | 105 | -7.40 | 2 | 10 | 24 | 34855 | 129 | 0.92 | 2 | 10 | 24 | 29959 | 21 | 0. | 2 | 10 | 24 | 30247 | 189 | 301.50 | 1 | 148.6 |
| 126 | 10 | 25 | 16902 | 30 | -22.54 | 2 | 10 | 25 | 11719 | 128 | 0.65 | 2 | 10 | 25 | 6823 | 20 | 0. | 2 | 10 | 25 | 7111 | 178 | 296.90 | 1 | 146.0 |
| 127 | 10 | 25 | 53766 | 0 | C. | 6 | 10 | 25 | 48582 | 129 | 0.92 | 2 | 10 | 25 | 43686 | 19 | 0. | 2 | 10 | 25 | 43974 | 143 | 281.90 | 1 | 690.0 |
| 128 | 10 | 26 | 30630 | 13 | -25.98 | 2 | 10 | 26 | 25446 | 127 | 0.37 | 2 | 10 | 26 | 20550 | 18 | 0. | 2 | 10 | 26 | 20838 | 94 | 260.80 | 1 | 152.4 |
| 129 | 10 | 27 | 7494 | 100 | -8.41 | 2 | 10 | 27 | 2310 | 127 | 0.37 | 2 | 10 | 26 | 57414 | 18 | 0. | 2 | 10 | 26 | 57702 | 56 | 243.20 | 1 | 151.6 |
| 130 | 10 | 27 | 44358 | 160 | 12.09 | 2 | 10 | 27 | 39174 | 129 | 0.92 | 2 | 10 | 27 | 34278 | 19 | 0. | 2 | 10 | 27 | 34566 | 46 | 237.80 | 1 | 145.0 |
| 131 | 10 | 28 | 21222 | 239 | 28.65 | 2 | 10 | 28 | 16038 | 126 | -0.09 | 2 | 10 | 28 | 11142 | 17 | 0. | 2 | 10 | 28 | 11430 | 67 | 248.40 | 1 | 144.7 |
| 132 | 10 | 28 | 58086 | 255 | 31.99 | 2 | 10 | 28 | 52902 | 125 | -0.18 | 2 | 10 | 28 | 48006 | 19 | 0. | 2 | 10 | 28 | 48294 | 126 | 275.00 | 1 | 147.0 |
| 133 | 10 | 29 | 34949 | 214 | 23.41 | 2 | 10 | 29 | 29765 | 124 | -0.45 | 2 | 10 | 29 | 24870 | 21 | 0. | 2 | 10 | 29 | 25158 | 183 | 299.00 | 1 | 143.0 |
| 134 | 10 | 30 | 11813 | 134 | 4.19 | 2 | 10 | 30 | 6629 | 123 | -0.73 | 2 | 10 | 30 | 1733 | 21 | 0. | 2 | 10 | 30 | 2021 | 195 | 304.00 | 1 | 145.0 |
| 135 | 10 | 30 | 48677 | 92 | -10.03 | 2 | 10 | 30 | 43493 | 127 | 0.37 | 2 | 10 | 30 | 38597 | 21 | 0. | 2 | 10 | 30 | 38885 | 195 | 304.00 | 1 | 145.1 |
| 136 | 10 | 31 | 25541 | 20 | -24.56 | 2 | 10 | 31 | 20357 | 131 | 1.47 | 2 | 10 | 31 | 15461 | 20 | 0. | 2 | 10 | 31 | 15750 | 169 | 293.00 | 1 | 147.9 |
| 137 | 10 | 32 | 2405 | 0 | 0. | 6 | 10 | 31 | 57221 | 128 | 0.65 | 2 | 10 | 31 | 52325 | 19 | 0. | 2 | 10 | 31 | 52613 | 116 | 270.60 | 1 | 690.0 |
| 138 | 10 | 32 | 39269 | 19 | -24.97 | 2 | 10 | 32 | 34085 | 129 | 0.92 | 2 | 10 | 32 | 29189 | 18 | 0. | 2 | 10 | 32 | 29477 | 66 | 247.90 | 1 | 146.3 |
| 139 | 10 | 33 | 16133 | 120 | -1.40 | 2 | 10 | 33 | 10949 | 130 | 1.19 | 2 | 10 | 33 | 6053 | 18 | 0. | 2 | 10 | 33 | 6341 | 47 | 238.30 | 1 | 147.1 |
| 140 | 10 | 33 | 52996 | 198 | 20.06 | 2 | 10 | 33 | 47812 | 124 | -0.45 | 2 | 10 | 33 | 42916 | 18 | 0. | 2 | 10 | 33 | 43204 | 58 | 244.00 | 1 | 148.0 |
| 141 | 10 | 34 | 29560 | 255 | 31.99 | 2 | 10 | 34 | 24676 | 126 | -0.09 | 2 | 10 | 34 | 19780 | 18 | 0. | 2 | 10 | 34 | 20068 | 89 | 258.40 | 1 | 146.2 |
| 142 | 10 | 35 | 6724 | 255 | 31.99 | 2 | 10 | 35 | 1540 | 126 | -0.09 | 2 | 10 | 34 | 56644 | 20 | 0. | 2 | 10 | 34 | 56932 | 152 | 285.80 | 1 | 144.7 |
| 143 | 10 | 35 | 43988 | 193 | 19.01 | 2 | 10 | 35 | 38404 | 125 | -0.18 | 2 | 10 | 35 | 33508 | 21 | 0. | 2 | 10 | 35 | 33796 | 190 | 301.90 | 1 | 143.2 |
| 144 | 10 | 36 | 20452 | 118 | -2.20 | 2 | 10 | 36 | 15268 | 125 | -0.18 | 2 | 10 | 36 | 10372 | 21 | 0. | 2 | 10 | 36 | 10660 | 195 | 304.00 | 1 | 145.8 |
| 145 | 10 | 36 | 57316 | 40 | -20.52 | 2 | 10 | 36 | 52132 | 130 | 1.19 | 2 | 10 | 36 | 47236 | 21 | 0. | 2 | 10 | 36 | 47524 | 195 | 304.00 | 1 | 142.0 |
| 146 | 10 | 37 | 34180 | 0 | 0. | 6 | 10 | 37 | 28996 | 131 | 1.47 | 2 | 10 | 37 | 24100 | 20 | 0. | 2 | 10 | 37 | 24388 | 161 | 289.60 | 1 | 690.0 |
| 147 | 10 | 38 | 11043 | 5 | -27.59 | 2 | 10 | 38 | 5859 | 127 | 0.37 | 2 | 10 | 38 | 963 | 18 | 0. | 2 | 10 | 38 | 1251 | 106 | 266.30 | 1 | 152.1 |
| 148 | 10 | 38 | 47907 | 78 | -12.85 | 2 | 10 | 38 | 42723 | 129 | 0.92 | 2 | 10 | 38 | 37827 | 18 | 0. | 2 | 10 | 38 | 38115 | 59 | 244.60 | 1 | 150.9 |
| 149 | 10 | 39 | 24771 | 138 | 5.80 | 2 | 10 | 39 | 19587 | 127 | 0.37 | 2 | 10 | 39 | 14691 | 22 | 0. | 2 | 10 | 39 | 14979 | 39 | 233.90 | 1 | 143.1 |
| 150 | 10 | 40 | 1635 | 223 | 25.29 | 2 | 10 | 39 | 56451 | 126 | -0.09 | 2 | 10 | 39 | 51555 | 18 | 0. | 2 | 10 | 39 | 51843 | 53 | 241.50 | 1 | 142.7 |

PAGE NO. 4 FILE NO. 1 DAY NO. 20

| RC | HR MN MSECS | A10 | IC | HR MN MSECS | A11 | IC | HR MN MSECS | A12 | IC | HR MN MSECS | A13 | IC | ALPHA |
|---|---|---|---|---|---|---|---|---|---|---|---|---|---|
| 151 | 10 40 38500 255 | 31.59 | 2 | 10 40 33315 124 | -0.45 | 2 | 10 40 28419 18 | C. | 2 | 10 40 28707 110 | 267.90 | 1 | 148.0 |
| 152 | 10 41 15362 233 | 27.39 | 2 | 10 41 10179 124 | -0.45 | 2 | 10 41 5283 20 | C. | 2 | 10 41 5571 170 | 293.40 | 1 | 144.3 |
| 153 | 10 41 52227 158 | 11.68 | 2 | 10 41 47043 124 | -0.45 | 2 | 10 41 42147 22 | C. | 2 | 10 41 42435 195 | 304.00 | 1 | 143.8 |
| 154 | 10 42 29090 111 | -5.00 | 2 | 10 42 23906 126 | -0.09 | 2 | 10 42 19010 21 | C. | 2 | 10 42 19298 195 | 304.00 | 1 | 145.6 |
| 155 | 10 43 5954 24 | -23.75 | 2 | 10 43 770 130 | 1.19 | 2 | 10 42 55875 20 | C. | 2 | 10 42 56162 181 | 298.20 | 1 | 144.7 |
| 156 | 10 43 42818 0 | 0. | 6 | 10 43 37634 129 | 0.92 | 2 | 10 43 32738 19 | C. | 2 | 10 43 33026 136 | 279.00 | 1 | 690.0 |
| 157 | 10 44 19682 4 | -27.79 | 2 | 10 44 14498 130 | 1.19 | 2 | 10 44 9602 18 | C. | 2 | 10 44 9890 82 | 255.20 | 1 | 148.2 |
| 158 | 10 44 56546 107 | -6.59 | 2 | 10 44 51362 129 | 0.92 | 2 | 10 44 46466 18 | C. | 2 | 10 44 46754 57 | 243.50 | 1 | 151.9 |
| 159 | 10 45 33410 192 | 16.70 | 2 | 10 45 28226 126 | -0.09 | 2 | 10 45 23330 18 | C. | 2 | 10 45 23618 55 | 242.70 | 1 | 148.4 |
| 160 | 10 46 10274 255 | 31.99 | 2 | 10 46 5090 126 | -0.09 | 2 | 10 46 194 18 | C. | 2 | 10 46 482 69 | 249.40 | 1 | 142.6 |
| 161 | 10 46 47137 255 | 31.99 | 2 | 10 46 41953 125 | -0.18 | 2 | 10 46 37057 19 | C. | 2 | 10 46 37345 128 | 275.80 | 1 | 147.3 |
| 162 | 10 47 24001 196 | 19.64 | 2 | 10 47 18817 124 | -0.45 | 2 | 10 47 13921 20 | C. | 2 | 10 47 14209 174 | 295.10 | 1 | 148.2 |
| 163 | 10 48 865 126 | 1.00 | 2 | 10 47 55681 126 | -0.09 | 2 | 10 47 50785 21 | C. | 2 | 10 47 51073 192 | 302.80 | 1 | 147.1 |
| 164 | 10 48 37729 52 | -18.10 | 2 | 10 48 32545 127 | 0.37 | 2 | 10 48 27649 20 | C. | 2 | 10 48 27937 194 | 303.60 | 1 | 142.7 |
| 165 | 10 49 14593 4 | -27.79 | 2 | 10 49 9409 131 | 1.47 | 2 | 10 49 4513 20 | C. | 2 | 10 49 4801 174 | 295.10 | 1 | 144.3 |
| 166 | 10 49 51457 9 | -26.78 | 2 | 10 49 46273 129 | 0.92 | 2 | 10 49 41377 19 | C. | 2 | 10 49 41665 120 | 272.40 | 1 | 153.2 |
| 167 | 10 50 28321 68 | -14.87 | 2 | 10 50 23137 131 | 1.47 | 2 | 10 50 18241 18 | C. | 2 | 10 50 18529 68 | 248.90 | 1 | 153.1 |
| 168 | 10 51 5184 128 | 1.80 | 2 | 10 51 0 128 | 0.65 | 2 | 10 50 55104 19 | C. | 2 | 10 50 55392 46 | 237.80 | 1 | 147.1 |
| 169 | 10 51 42048 210 | 22.57 | 2 | 10 51 36864 125 | -0.18 | 2 | 10 51 31968 18 | C. | 2 | 10 51 32256 50 | 239.90 | 1 | 143.2 |
| 170 | 10 52 18912 140 | 6.59 | 2 | 10 52 13728 125 | -0.18 | 2 | 10 52 8832 18 | C. | 2 | 10 52 9120 95 | 261.20 | 1 | 169.2 |
| 171 | 10 52 55776 126 | 1.00 | 2 | 10 52 50592 127 | 0.37 | 2 | 10 52 45696 18 | C. | 2 | 10 52 45984 99 | 263.00 | 1 | 172.6 |
| 172 | 10 53 32640 126 | 1.00 | 2 | 10 53 27456 127 | 0.37 | 2 | 10 53 22560 18 | C. | 2 | 10 53 22848 99 | 263.00 | 1 | 172.6 |
| 173 | 10 54 9504 126 | 1.00 | 2 | 10 54 4320 127 | 0.37 | 2 | 10 53 59424 18 | C. | 2 | 10 53 59712 99 | 263.00 | 1 | 172.6 |
| 174 | 10 54 46368 125 | 0.59 | 2 | 10 54 41184 127 | 0.37 | 2 | 10 54 36288 18 | C. | 2 | 10 54 36576 99 | 263.00 | 1 | 172.6 |
| 175 | 10 55 23231 126 | 1.00 | 2 | 10 55 18047 127 | 0.37 | 2 | 10 55 13151 18 | C. | 2 | 10 55 13439 99 | 263.00 | 1 | 172.6 |
| 176 | 10 56 95 126 | 1.00 | 2 | 10 55 54911 127 | 0.37 | 2 | 10 55 50015 18 | C. | 2 | 10 55 50303 99 | 263.00 | 1 | 172.6 |
| 177 | 10 56 36959 126 | 1.00 | 2 | 10 56 31775 127 | 0.37 | 2 | 10 56 26879 18 | C. | 2 | 10 56 27167 99 | 263.00 | 1 | 172.6 |
| 178 | 10 57 13823 126 | 1.00 | 2 | 10 57 8639 127 | 0.37 | 2 | 10 57 3743 18 | C. | 2 | 10 57 4031 99 | 263.00 | 1 | 172.6 |
| 179 | 10 57 50687 125 | 0.59 | 2 | 10 57 45503 127 | 0.37 | 2 | 10 57 40607 18 | C. | 2 | 10 57 40895 99 | 263.00 | 1 | 172.6 |
| 180 | 10 58 27551 126 | 1.00 | 2 | 10 58 22367 127 | 0.37 | 2 | 10 58 17471 18 | C. | 2 | 10 58 17759 99 | 263.00 | 1 | 172.6 |
| 181 | 10 59 4414 126 | 1.00 | 2 | 10 58 59231 127 | 0.37 | 2 | 10 58 54335 18 | C. | 2 | 10 58 54623 99 | 263.00 | 1 | 172.6 |
| 182 | 10 59 41278 126 | 1.00 | 2 | 10 59 36094 127 | 0.37 | 2 | 10 59 31198 18 | C. | 2 | 10 59 31486 98 | 262.60 | 1 | 172.2 |
| 183 | 11 0 18142 126 | 1.00 | 2 | 11 0 12958 127 | 0.37 | 2 | 11 0 8062 18 | C. | 2 | 11 0 8350 99 | 263.00 | 1 | 172.6 |
| 184 | 11 0 55006 125 | 0.59 | 2 | 11 0 49822 127 | 0.37 | 2 | 11 0 44926 18 | C. | 2 | 11 0 45214 99 | 263.00 | 1 | 172.6 |
| 185 | 11 1 31870 126 | 1.00 | 2 | 11 1 26686 127 | 0.37 | 2 | 11 1 21790 18 | C. | 2 | 11 1 22078 99 | 263.00 | 1 | 172.6 |
| 186 | 11 2 8734 126 | 1.00 | 2 | 11 2 3550 127 | 0.37 | 2 | 11 1 58654 18 | C. | 2 | 11 1 58942 99 | 263.00 | 1 | 172.6 |
| 187 | 11 2 45598 126 | 1.00 | 2 | 11 2 40414 127 | 0.37 | 2 | 11 2 35518 18 | C. | 2 | 11 2 35806 99 | 263.00 | 1 | 172.6 |
| 188 | 11 3 22461 126 | 1.00 | 2 | 11 3 17278 127 | 0.37 | 2 | 11 3 12382 18 | C. | 2 | 11 3 12670 99 | 263.00 | 1 | 172.6 |
| 189 | 11 3 59325 125 | 0.59 | 2 | 11 3 54141 127 | 0.37 | 2 | 11 3 49245 18 | C. | 2 | 11 3 49533 99 | 263.00 | 1 | 172.6 |
| 190 | 11 4 36189 126 | 1.00 | 2 | 11 4 31005 127 | 0.37 | 2 | 11 4 26109 18 | C. | 2 | 11 4 26397 99 | 263.00 | 1 | 172.6 |
| 191 | 11 5 13053 126 | 1.00 | 2 | 11 5 7869 127 | 0.37 | 2 | 11 5 2973 18 | C. | 2 | 11 5 3261 99 | 263.00 | 1 | 172.6 |
| 192 | 11 5 49917 126 | 1.00 | 2 | 11 5 44733 127 | 0.37 | 2 | 11 5 39837 18 | C. | 2 | 11 5 40125 99 | 263.00 | 1 | 172.6 |
| 193 | 11 6 26781 126 | 1.00 | 2 | 11 6 21597 127 | 0.37 | 2 | 11 6 16701 18 | C. | 2 | 11 6 16989 99 | 263.00 | 1 | 172.6 |
| 194 | 11 7 3645 125 | 0.59 | 2 | 11 6 58461 127 | 0.37 | 2 | 11 6 53565 18 | C. | 2 | 11 6 53853 99 | 263.00 | 1 | 172.6 |
| 195 | 11 7 40508 126 | 1.00 | 2 | 11 7 35324 127 | 0.37 | 2 | 11 7 30429 18 | C. | 2 | 11 7 30717 98 | 262.60 | 1 | 172.2 |
| 196 | 11 8 17372 126 | 1.00 | 2 | 11 8 12188 127 | 0.37 | 2 | 11 8 7292 18 | C. | 2 | 11 8 7580 99 | 263.00 | 1 | 172.6 |
| 197 | 11 8 54236 126 | 1.00 | 2 | 11 8 49052 127 | 0.37 | 2 | 11 8 44156 18 | C. | 2 | 11 8 44444 99 | 263.00 | 1 | 172.6 |
| 198 | 11 9 31100 126 | 1.00 | 2 | 11 9 25916 127 | 0.37 | 2 | 11 9 21020 18 | C. | 2 | 11 9 21308 99 | 263.00 | 1 | 172.6 |
| 199 | 11 10 7964 125 | 0.59 | 2 | 11 10 2780 126 | -0.09 | 2 | 11 9 57884 18 | C. | 2 | 11 9 58172 99 | 263.00 | 1 | 173.1 |
| 200 | 11 10 44828 126 | 1.00 | 2 | 11 10 39644 128 | 0.65 | 2 | 11 10 34748 18 | C. | 2 | 11 10 35036 99 | 263.00 | 1 | 172.3 |

# APPENDIX C

The calibration matrices used were, essentially, sent to us through private correspondence, by W. E. Kesler of Scientific Experiments, OGO Project Office of TRW. A brief discussion on these can be found on publication X-420-62-208A of October 1, 1965 prepared by Goddard Space Flight Center. Through indications from the data and private correspondence it was agreed upon that the limit switch on the solar panels allowed them to go up to 300 degrees as opposed to the 280 degrees which was the intended limit. We extrapolated the A-13 - Hi calibration to that point.

The full calibration matrices appear on pages C.2 - C.9.

| | 1 | 2 | 3 | 4 | 5 | 6 | 7 | 8 | 9 | C.2 10 |
|---|---|---|---|---|---|---|---|---|---|---|
| 0 | 000.00 | 000.00 | 000.00 | 000.00 | 000.00 | 000.00 | 000.00 | 000.00 | 000.00 | 000.00 |
| 1 | 000.00 | 000.00 | 000.00 | 000.00 | 000.00 | 000.00 | 000.00 | 000.00 | 000.00 | 000.00 |
| 2 | 000.00 | 000.00 | 000.00 | 000.00 | 000.00 | 000.00 | 000.00 | 000.00 | 000.00 | 000.00 |
| 3 | 000.00 | 000.00 | 000.00 | 000.00 | 000.00 | 000.00 | 000.00 | -15.99 | -15.84 | -15.67 |
| 4 | -15.51 | -15.35 | -15.19 | -15.02 | -14.86 | -14.69 | -14.53 | -14.37 | -14.21 | -14.06 |
| 5 | -13.88 | -13.72 | -13.56 | -13.39 | -13.23 | -13.07 | -12.91 | -12.74 | -12.58 | -12.42 |
| | -12.26 | -12.09 | -11.93 | -11.77 | -11.60 | -11.44 | -11.28 | -11.12 | -10.95 | -10.79 |
| | -10.63 | -10.47 | -10.30 | -10.14 | -9.98 | -9.81 | -9.65 | -9.49 | -9.33 | -9.16 |
| | -9.00 | -8.80 | -8.60 | -8.41 | -8.21 | -8.02 | -7.82 | -7.63 | -7.43 | -7.24 |
| | -7.04 | -6.84 | -6.65 | -6.45 | -6.26 | -6.06 | -5.87 | -5.67 | -5.48 | -5.28 |
| | -5.08 | -4.89 | -4.69 | -4.49 | -4.30 | -4.11 | -3.91 | -3.72 | -3.52 | -3.32 |
| | -3.13 | -2.93 | -2.74 | -2.54 | -2.35 | -2.15 | -1.96 | -1.76 | -1.56 | -1.37 |
| | -1.17 | -0.98 | -0.78 | -0.59 | -0.39 | -0.19 | 0.01 | 0.39 | 0.68 | 0.96 |
| | 1.24 | 1.51 | 1.79 | 2.07 | 2.35 | 2.63 | 2.91 | 3.19 | 3.46 | 3.74 |
| | 4.02 | 4.29 | 4.49 | 4.67 | 4.84 | 5.00 | 5.17 | 5.34 | 5.51 | 5.67 |
| | 5.84 | 6.01 | 6.18 | 6.34 | 6.51 | 6.68 | 6.85 | 7.01 | 7.18 | 7.35 |
| | 7.52 | 7.69 | 7.85 | 8.02 | 8.19 | 8.36 | 8.52 | 8.69 | 8.86 | 9.03 |
| | 9.19 | 9.36 | 9.53 | 9.69 | 9.86 | 10.03 | 10.20 | 10.37 | 10.54 | 10.70 |
| | 10.87 | 11.04 | 11.21 | 11.37 | 11.54 | 11.71 | 11.88 | 12.04 | 12.21 | 12.38 |
| | 12.55 | 12.71 | 12.88 | 13.05 | 13.22 | 13.39 | 13.55 | 13.72 | 13.89 | 14.06 |
| | 14.22 | 14.39 | 14.56 | 14.73 | 14.89 | 15.06 | 15.23 | 15.39 | 15.56 | 15.73 |
| | 15.90 | 16.00 | 16.07 | 16.14 | 16.21 | 16.29 | 16.36 | 16.43 | 16.50 | 0.00 |
| | 000.00 | 000.00 | 000.00 | 000.00 | 000.00 | 000.00 | 000.00 | 000.00 | 000.00 | 000.00 |
| | 000.00 | 000.00 | 000.00 | 000.00 | 000.00 | 000.00 | 000.00 | 000.00 | 000.00 | 000.00 |
| | 000.00 | 000.00 | 000.00 | 000.00 | 000.00 | 000.00 | 000.00 | 000.00 | 000.00 | 000.00 |
| | 000.00 | 000.00 | 000.00 | 000.00 | 000.00 | 000.00 | 000.00 | 000.00 | 000.00 | 000.00 |

A-10 FINE